Hindawi
International Journal of Antennas and Propagation
Volume 2017, Article ID 9482979, 8 pages
https://doi.org/10.1155/2017/9482979

Research Article

Design of a Microstrip Series Power Divider for Sequentially Rotated Nonuniform Antenna Array

Daniele Inserra, Wei Hu, and Guangjun Wen

School of Communications & Information Technology, University of Electronic Science and Technology of China, Chengdu, China

Correspondence should be addressed to Daniele Inserra; inserradaniele@uestc.edu.cn

Received 2 December 2016; Accepted 10 January 2017; Published 26 January 2017

Academic Editor: N. Nasimuddin

This paper deals with the design of a microstrip series power divider for circularly polarized sequential rotational antenna array. The theoretical description of the design is firstly proposed, comprising the cases of nonuniform weighted antenna arrays. A more flexible open octagon shape instead of the classical open ring is suggested, highlighting benefits in the case of nonuniform power distribution. A design example of an ultra-high frequency (UHF) band 4×4 sequentially rotated Tschebischeff antenna array finally demonstrates the effectiveness of the proposed implementation.

1. Introduction

Circularly polarized (CP) patch antennas have gained considerable interest due to their main advantage of being insensitive to depolarization [1, 2]. For these reasons, many applications such as satellite, radar tracking, and mobile communication systems rely on these kinds of antennas. Further, the uses of microstrip technology to implement CP antenna arrays have made these antennas an excellent candidate owing to their light weight, low profile, ease of fabrication, with low manufacturing cost, and ease of integration [3, 4].

The design of a single CP antenna intrinsically has narrow impedance and axial ratio (AR) bandwidth. However, many applications demand good performance for both impedance and AR over a wide frequency bandwidth. Sequential rotation (SR) technique has been extensively used to improve impedance and AR performances in array design. The mechanism of SR technique has been theoretically and experimentally analyzed [5–9], and some useful design principles have also been summarized. The designated array element can be either linearly polarized (LP) [10] or CP type. If an LP array element is used, the design process of the array antenna (with sequential rotation technique) will be easier than that for the CP array element type. This is because the process of adjusting the CP performance of each array element can be avoided. However, the resulting compound array gain will be lower than the array using the CP element [3].

It has been proved in [11] that the CP bandwidth in the axial broadside direction can be very wide if the feeding network is able to preserve the correct amplitude and phase over the frequency. However, owing to magnitude errors, phase errors, impedance mismatch, and mutual coupling, the practical CP bandwidth is limited by the feeding network and/or the radiating elements performance. Consequently, considerable investigations have been carried out for the simple and compact sequential phase (SP) feed structures.

In [12], Evans et al. describe the use of a series feed network to provide appropriate phase shifting and power splitting among the radiating elements. They have implemented such a feed network with an open ring shaped structure. The same implementation is also used in [4, 13, 14], even if no theoretical elements for the series feed network design are provided, except in [4], where only the uniform weighted antenna array case is treated.

Other feeding structures are also suggested in [6, 15–17] for SR antenna arrays. In particular, in [16] different feeding implementations are presented and compared. It is shown that good performance can be achieved with a

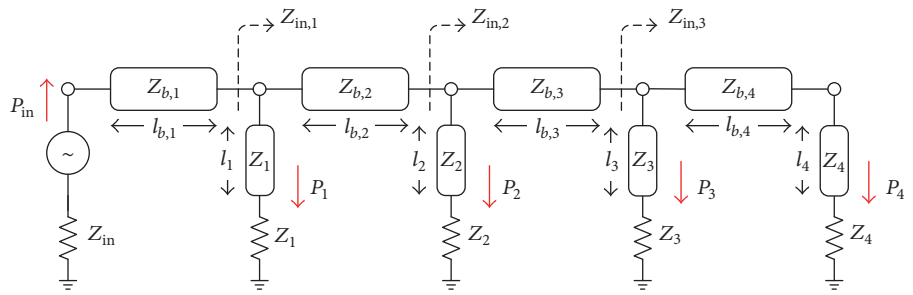

Figure 1: Equivalent circuit of the series power divider.

hybrid ring feeding network. Nonetheless, the high dielectric permittivity and the thick substrate height employed allow for realizing more complex feeding structures with compact size due to the very short wavelength. This is not the case of common used substrate materials, where compact feeding implementations are preferred. Among the cited, the open ring shaped structure offers compactness and simplicity characteristics.

In this paper, the theoretical design of a series power divider for the generic output power distribution case is presented. To the best of the authors' knowledge, a theoretical analysis of the series power divider with generic output power distribution is not present in the literature. A more flexible open octagon shape instead of the classical open ring implementation is proposed. This modification provides better results because of the flexibility to realize different quarter wave transformer lengths, which better address the case of different quarter wave transformer characteristic impedance. Simulation results are presented to confirm these benefits. Finally, the design of an ultra-high frequency (UHF) band 4 × 4 SR Tschebischeff antenna array for radio-frequency identification (RFID) applications is described, and the comparison between simulation and measurement results validates the proposed work.

This paper is organized as follows. The design of a microstrip series power divider is theoretically treated in Section 2. Section 3 describes the implementation drawbacks of the classical open ring shape divider and the new open octagon implementation. The 4 × 4 antenna array design is reported in Section 4. Finally, conclusions follow.

2. Theoretical Design

An equivalent circuit of the series power divider is depicted in Figure 1, with generic power distribution P_i, $i \in \{1, \ldots, 4\}$, and load impedance Z_i, $i \in \{1, \ldots, 4\}$. The four output ports are connected through four quarter wave impedance transformers with characteristic impedance $Z_{b,i}$, $i \in \{1, \ldots, 4\}$, and branch lengths $l_{b,i}$, $i \in \{1, \ldots, 4\}$. Finally, four adapted lines of length l_i, $i \in \{1, \ldots, 4\}$, and characteristic impedance Z_i, $i \in \{1, \ldots, 4\}$, are used to provide a generic phase contribution $\phi_i = (2\pi/\lambda_g)l_i$, $i \in \{1, \ldots, 4\}$. Considering the case of unequal power divider, calling the power at the output ports P_1, P_2, P_3, and P_4, the following *power relations* can be derived:

$$Z_{\text{in},1} = Z_1 \frac{P_1}{P_{\text{in}}},$$
$$Z_{\text{in},2} = Z_2 \frac{P_2}{P_{\text{in}-P_1}}, \tag{1}$$
$$Z_{\text{in},3} = Z_3 \frac{P_3}{P_{\text{in}-P_1-P_2}}.$$

Furthermore, in order to guarantee impedance matching at each intersection of the series divider, the following *impedance relations* have to be respected:

$$Z_{\text{in},1} = \frac{Z_1 Z_{b,2}^2}{Z_1 Z_{\text{in},2} + Z_{b,2}^2},$$
$$Z_{\text{in},2} = \frac{Z_2 Z_{b,3}^2}{Z_2 Z_{\text{in},3} + Z_{b,3}^2}, \tag{2}$$
$$Z_{\text{in},3} = \frac{Z_3 Z_{b,4}^2}{Z_3 Z_4 + Z_{b,4}^2}.$$

Finally, the first quarter wave impedance transformer is only used to match the source impedance to the series divider input impedance, and then

$$Z_{\text{in}} = \frac{Z_{b,1}^2}{Z_{\text{in},1}}. \tag{3}$$

Equations in (2) can be elaborated to obtain closed-form expressions of the four branches characteristic impedance

$$Z_{b,1} = \sqrt{Z_{\text{in}} Z_{\text{in},1}},$$
$$Z_{b,2} = \sqrt{\frac{Z_{\text{in},1} Z_{\text{in},2} Z_1}{Z_1 - Z_{\text{in},1}}},$$
$$Z_{b,3} = \sqrt{\frac{Z_{\text{in},2} Z_{\text{in},3} Z_2}{Z_2 - Z_{\text{in},2}}}, \tag{4}$$
$$Z_{b,4} = \sqrt{\frac{Z_{\text{in},3} Z_3 Z_4}{Z_3 - Z_{\text{in},3}}}.$$

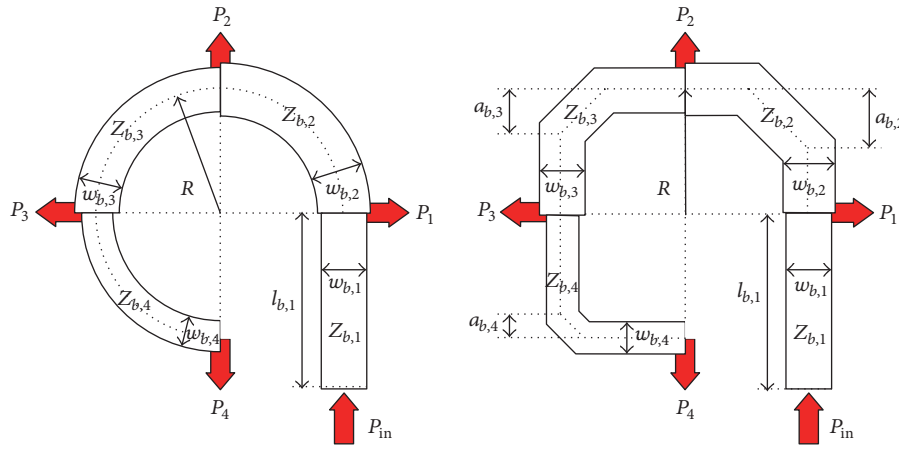

FIGURE 2: Open ring and open octagon implementations of the series power divider.

From the above equations, a design procedure can be summarized:

(1) After defining the power coefficients P_i, $i \in \{1, \ldots, 4\}$, and the phases ϕ_i, $i \in \{1, \ldots, 4\}$, according to an antenna array synthesis procedure, the impedance $Z_{\text{in},i}$, $i \in \{1, \ldots, 3\}$, can be calculated as in (1).

(2) From (4), the characteristic impedances of the branch lines $Z_{b,i}$, $i \in \{1, \ldots, 4\}$, are determined.

(3) The adapted lines lengths l_i, $i \in \{1, \ldots, 4\}$, are calculated in order to provide a different phase contribution ϕ_i, $i \in \{1, \ldots, 4\}$, according to the antenna array synthesis parameters.

3. Implementation of the Series Divider

A common microstrip implementation of the series divider has an open ring shape [4, 12–14], and it is depicted on the left side of Figure 2 for a right hand circular polarization (RHCP) antenna array. The implementation procedure of the open ring series divider basically consists in the following steps:

(1) The microstrip branches widths $w_{b,i}$, $i \in \{1, \ldots, 4\}$, are calculated in order to yield the branches characteristic impedance $Z_{b,i}$, $i \in \{1, \ldots, 4\}$, previously designed according to the series divider design procedure described above.

(2) The radius $R = \lambda_g/2\pi$ is optimized to guarantee 90 deg phase differences between consecutive output ports.

(3) The output phase contributions ϕ_i, $i \in \{1, \ldots, 4\}$, are tuned by varying the microstrip line lengths l_i, $i \in \{1, \ldots, 4\}$ (the widths of the output microstrip lines are calculated in order to yield the impedance Z_i, $i \in \{1, \ldots, 4\}$).

(4) The first branch length $l_{b,1}$ is finally optimized to achieve the minimum input return loss.

It should be noted that, according to [18], the effective dielectric constant of a microstrip line is a function of the microstrip width, that is, the impedance value; for this reason, each characteristic impedance corresponds to a specific value of the propagation constant, and for this reason, the length of each 90 deg shift branch ($l_{b,i}$, $i \in \{1, \ldots, 4\}$) has to be appropriately adjusted. The open ring implementation does not allow for adjusting each branch length since there is only one parameter, that is, the radius R, which fixes the branches length.

Thus, a different implementation of the series power divider is suggested in this work. The open ring is replaced with an open octagon, where the lengths of the three 45 deg edges are individually adjusted through the parameters $a_{b,i}$, $i \in \{2, \ldots, 4\}$, in order to better regulate the branch phase shifts (the three 45 deg edges can be also substituted with a curving line). This implementation is depicted on the right side of Figure 2. A new implementation procedure is herein described:

(1) The microstrip branches widths $w_{b,i}$, $i \in \{1, \ldots, 4\}$, are calculated as in the open ring implementation procedure.

(2) The radius $R = \lambda_g/2\pi$ is firstly optimized to achieve the minimum 90 deg branch phase error between consecutive output ports with $a_{b,i}$, $i \in \{2, \ldots, 4\}$, initially set as $a_{b,i} = R((2 - \pi/2)/(2 - \sqrt{2}))$, $i \in \{2, \ldots, 4\}$ (in this way, the branches have the same length as in the open ring implementation).

(3) The branch lengths $l_{b,i}$, $i \in \{1, \ldots, 4\}$, are individually optimized by varying the parameters $a_{b,i}$, $i \in \{2, \ldots, 4\}$, to minimize the 90 deg branch phase error; in this case, the radius R can also be modified for fine tuning purpose.

(4) The output line lengths l_i, $i \in \{1, \ldots, 4\}$, are tuned as in the open ring implementation procedure.

(5) The first branch length $l_{b,1}$ is finally optimized to yield the minimum input return loss.

It should be noted that the open octagon implementation introduces some new degrees of freedom; this is the reason

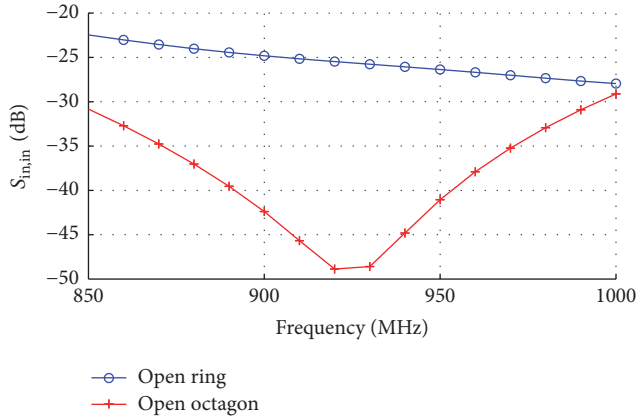

FIGURE 3: Nonuniform series divider $S_{in,in}$ results for both open ring and open octagon implementations.

why the radius R can be modified to better comply with the 90 deg phase tuning step.

Let us now consider the implementation of a nonuniform series divider for UHF applications. The microstrip divider is designed on a glass reinforced hydrocarbon and ceramic dielectric named S7136, with dielectric constant $\varepsilon_r = 3.52$, loss tangent $\tan\delta = 0.0035$, and thickness $h = 1.524$ mm. The working frequency is selected as 920 MHz. An input impedance of $Z_{in} = 50\,\Omega$ is assumed, while the output impedance is taken as $Z_i = 100\,\Omega$, $i \in \{1, \ldots, 4\}$. The power divider is simulated using the Ansoft HFSS commercial software [19], which is based on the finite element method. The output normalized power values are assumed as $P_1 = 0.6847$, $P_2 = 0.1260$, $P_3 = 0.0294$, and $P_4 = 0.1598$, with relative phase 0 deg. The open ring and the open octagon implementations are designed according to the procedures described above. Design values for the open ring are $R = 30.2$ mm, $w_{b,1} = 5.77$ mm, $w_{b,2} = 6.28$ mm, $w_{b,3} = 3.36$ mm, $w_{b,4} = 0.78$ mm, $l_{b,1} = 48.0$ mm. For the open octagon, instead, design values are $R = 29.0$ mm, $w_{b,1} = 5.77$ mm, $w_{b,2} = 6.28$ mm, $w_{b,3} = 3.36$ mm, $w_{b,4} = 0.78$ mm, $l_{b,1} = 53.9$ mm, $a_{b,2} = 12.1$ mm, $a_{b,3} = 15.4$ mm, $a_{b,4} = 18.1$ mm. Simulation results for both of the implementations are shown in Figures 3 and 4, while the achieved power and relative phase at the frequency of interest are reported in Table 1.

In this case, the open ring implementation cannot be optimized to have three 90 deg phase differences; this affects the input return loss performance, whose minimum does not correspond to the 90 deg phase difference error minimization situation (as shown in Figure 3). In the open octagon implementation, instead, the branch lengths can be singularly adjusted, and for this reason this implementation provides better performance. A minimum $S_{in,in} = -48.9$ dB is obtained at the center frequency, with very low phase and power mean errors as depicted in Figure 4. It should be noted that the length of the first branch $l_{b,1}$ is longer than the required to achieve 90 deg phase shift. This is because the input quarter wave transformer is also compensating the step in width discontinuity effects among the different width branches.

TABLE 1: Nonuniform series divider design results.

Parameter	Open ring	Open octagon
$S_{in,in}$	−25.5 dB	−48.9 dB
P_1	0.6653	0.6697
P_2	0.1276	0.1277
P_3	0.0324	0.0301
P_4	0.1644	0.1645
$\phi_{1,2}$	86.3 deg	89.6 deg
$\phi_{2,3}$	86.8 deg	90.3 deg
$\phi_{3,4}$	92.7 deg	89.9 deg

TABLE 2: Amplitude and phase feeding values for the antenna elements.

Antenna	Amplitude	Phase [deg]
1	0.0074	180 − 21.6
2	0.0315	270 − 21.6
3	0.0315	180 − 21.6
4	0.0074	270 − 21.6
5	0.0400	90 − 7.2
6	0.1712	−7.2
7	0.1712	90 − 7.2
8	0.0400	−7.2
9	0.0400	180 + 7.2
10	0.1712	270 + 7.2
11	0.1712	180 + 7.2
12	0.0400	270 + 7.2
13	0.0074	90 + 21.6
14	0.0315	21.6
15	0.0315	90 + 21.6
16	0.0074	21.6

4. UHF Band 4 × 4 CP Antenna Array

In this section, the design of UHF band 4×4 SR antenna array for RFID applications with central frequency 922.5 MHz is proposed. The antenna array weights were Tschebischeff distributed (the design sidelobe levels were 30 dB and 25 dB for the x- and y-axes, respectively, while the interelement distances were chosen as $d_x = 0.48\lambda_0$ and $d_y = 0.45\lambda_0$) [20], and a −5 deg steering elevation angle was also introduced. The amplitude and phase feeding values of each antenna element are reported in Table 2. The feeding network was designed with two levels of power distribution: a first level uniform series divider F_0 feeds four 2 × 2 subarrays; each subarray has a second level nonuniform series divider F_i, $i \in \{1, \ldots, 4\}$, which is connected to the antenna elements. The steering elevation angle was achieved by modifying the length of the output lines for both the first level feeding network (additional lengths Δw_i, $i \in \{1, \ldots, 4\}$) and the second level feeding network (additional lengths $l_i = 11.5$ mm for the antenna elements $\{1, 2, 3, 4, 9, 10, 11, 12\}$). A design scheme is reported in Figure 5, while the design parameters, obtained with the procedure described above, are listed in Table 3.

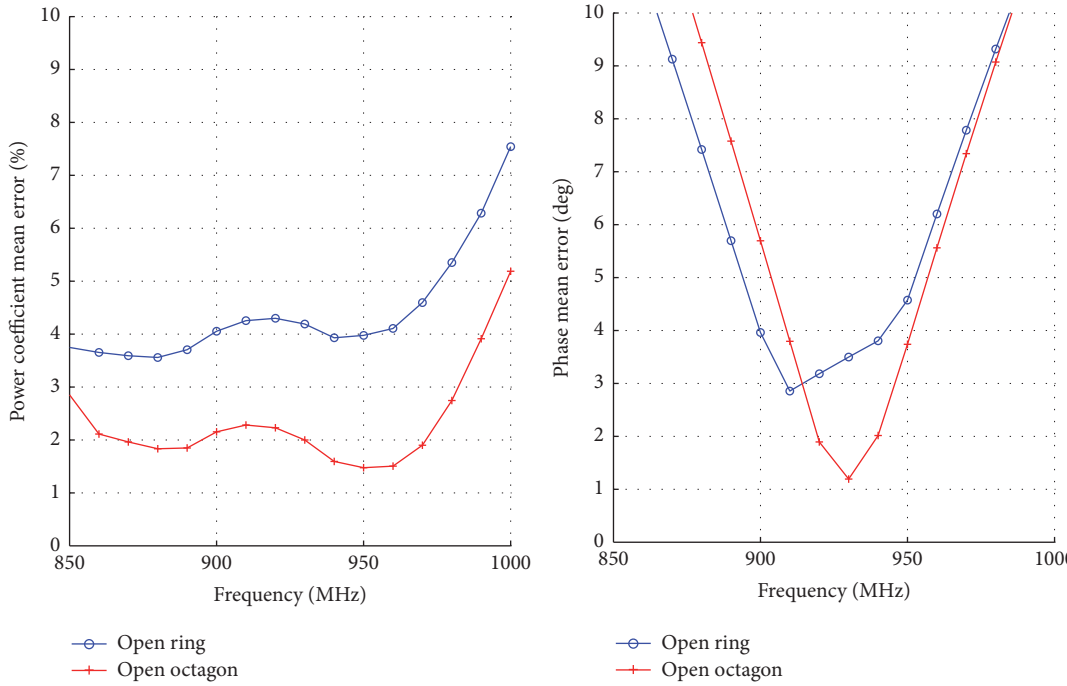

Figure 4: Nonuniform series divider power coefficient and phase mean errors for both open ring and open octagon implementations.

Table 3: Design parameters (measurement unit is mm).

Parameter	F_0	F_1	F_2	F_3	F_4
R	29.5	25.5	25.5	25.5	25.5
$w_{b,1}$	6.93	2.13	2.13	2.13	2.13
$w_{b,2}$	9.04	1.32	1.69	1.32	1.69
$w_{b,3}$	5.11	5.79	8.83	5.79	8.83
$w_{b,4}$	1.46	5.09	6.02	5.09	6.02
$a_{b,2}$	20.3	0.7	1.4	0.7	1.4
$a_{b,3}$	18.4	5.2	6.5	4.8	6.5
$a_{b,4}$	14.5	5.3	5.5	5.0	5.5
$l_{b,1}$	45.4	52.0	52.5	52.9	53.4
Δw_1	18.5	n.a.	n.a.	n.a.	n.a.
Δw_2	10.0	n.a.	n.a.	n.a.	n.a.
Δw_3	31.0	n.a.	n.a.	n.a.	n.a.
Δw_4	25.0	n.a.	n.a.	n.a.	n.a.

The single antenna element was $L = 86.4$ mm squared patch antenna with trimmed corners (8.8 mm and 5.5 mm corner truncations). A quarter wave impedance transformer of length 57.1 mm and width 0.5 mm provides impedance matching between the antenna and the feeding network. A coaxial feeding method was assumed, with input impedance value $Z_{\text{in}} = 50\,\Omega$, while the single antenna impedance was chosen as 80 Ω. The antenna array was designed on a S7136 substrate as in Section 3.

Theoretical design, simulated performance, and measurement results are compared in Figures 6, 7, 8, 9, 10, 11, and 12. Good correspondence between simulation and measurement results can be observed, even if few discrepancies arise due to mutual coupling among the antennas (the interelement distances are relatively small); in fact, mutual coupling modifies the input impedance of the antennas, and this effect has an impact on the feeding network performance, which is designed to drive perfect 80 Ω loads. Nonetheless, AR is lower than 2 dB within 20 MHz bandwidth and also within a broad angles set as it can be verified by Figures 8, 9, and 10, and this confirms that good 90 deg phase shift performance is achieved with the proposed implementation. For what the radiation pattern is concerned (Figures 11 and 12), differences between simulation and measurement results are negligible up to −20 dB of normalized power (except a little reduction of V plane radiation pattern beamwidth for negative elevation angles), and this also proves that both amplitude and phase synthesis are correctly implemented with the proposed method.

5. Conclusions

In this paper, the theoretical design of a generic microstrip series power divider is presented. The description is focused on the design of the series divider for CP SR antenna array. Particularly, the generic case of unequal output power and unequal output impedance is treated, which allows for designing nonuniform weighted antenna array. A more flexible open octagon shape instead of the classical open ring is suggested, highlighting benefits in the case of nonuniform power distribution. This modification provides better results because of the flexibility to realize different quarter wave transformer lengths, which better address the case of different quarter wave transformer characteristic impedance. A design example of UHF band 4 × 4 SR Tschebischeff antenna array

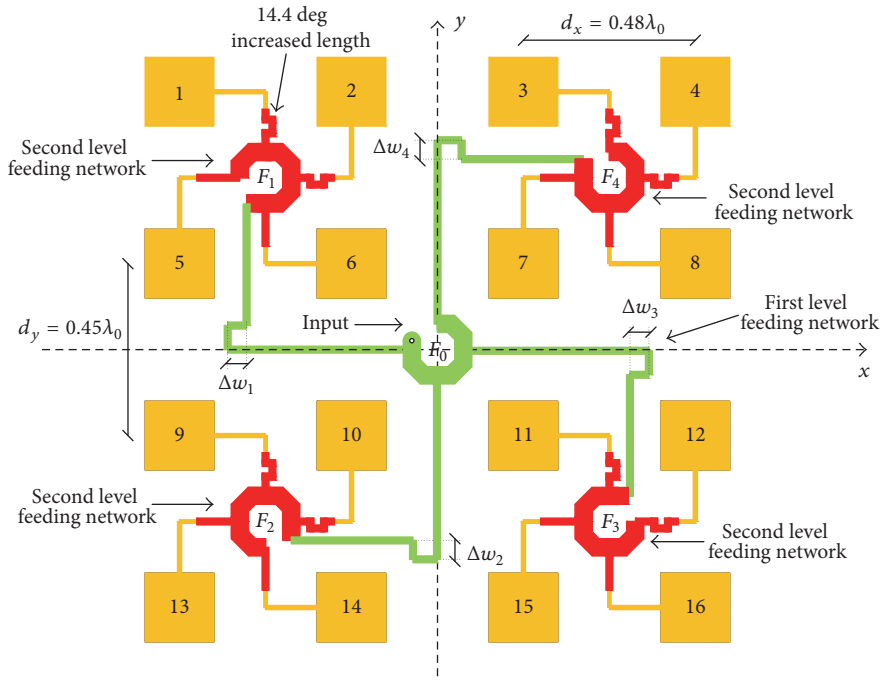

Figure 5: 4 × 4 antenna array design scheme.

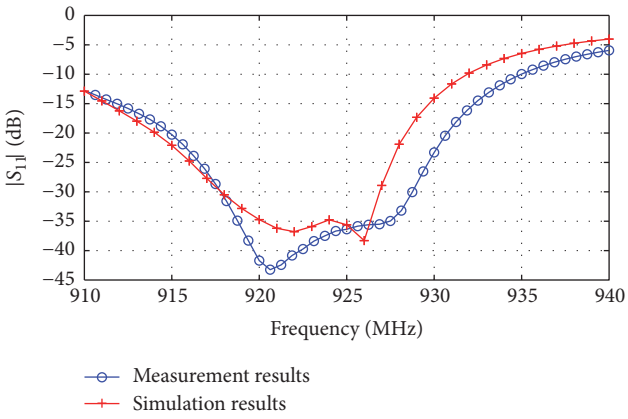

Figure 6: S_{11} of the 4 × 4 SR antenna array.

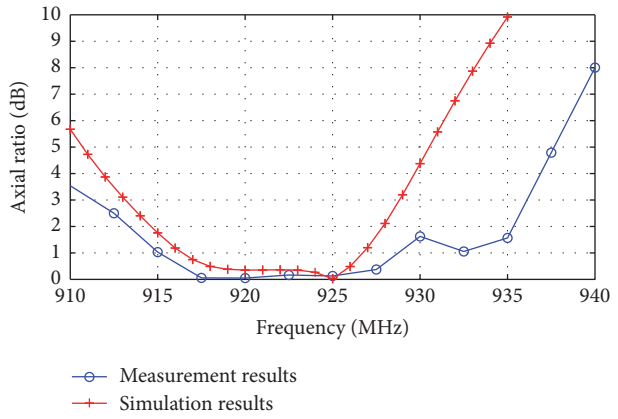

Figure 8: AR of the 4 × 4 SR antenna array.

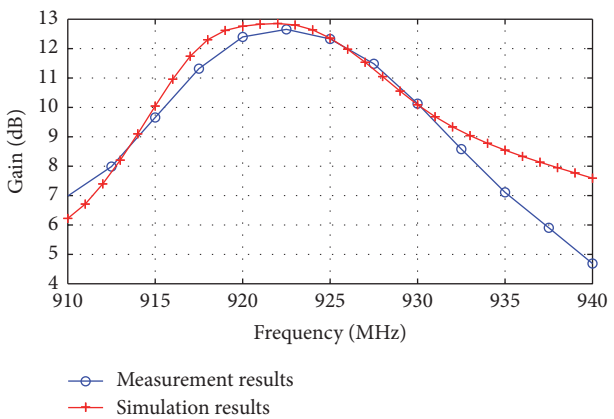

Figure 7: Broadside gain of the 4 × 4 SR antenna array.

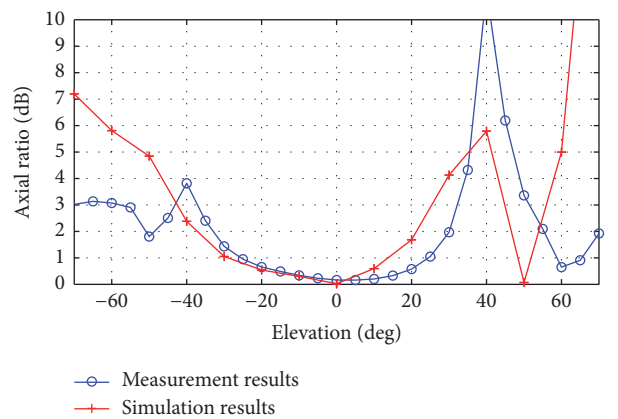

Figure 9: H plane AR as function of elevation angle at 922.5 MHz.

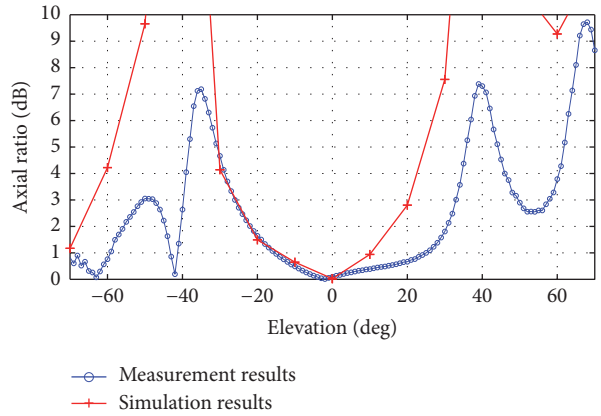

Figure 10: V plane AR as function of elevation angle at 922.5 MHz.

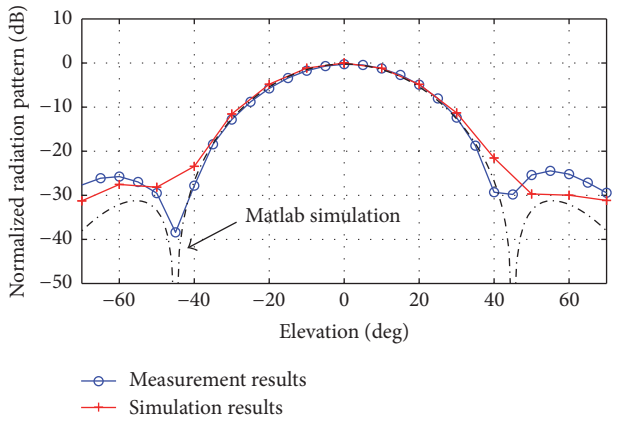

Figure 11: H plane radiation pattern at 922.5 MHz.

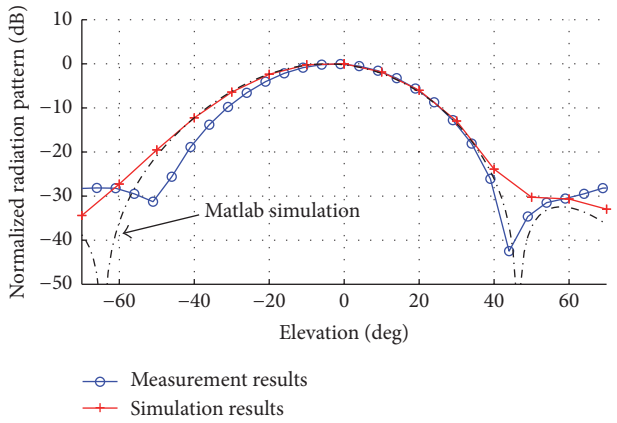

Figure 12: V plane radiation pattern at 922.5 MHz.

demonstrates the effectiveness of the proposed design implementation. Measurement reveals that AR is lower than 2 dB within 20 MHz bandwidth and also within a broad angles set; this confirms that good 90 deg phase shift performance is achieved with the proposed implementation. Furthermore, comparison between simulated and measured radiation pattern proves that both amplitude and phase synthesis are correctly implemented with the proposed method.

Competing Interests

The authors declare that there is no conflict of interests regarding the publication of this paper.

Acknowledgments

Authors acknowledge that part of the work herein presented was funded by National Natural Science Foundation of China under Project Contract no. 6137104, Guangdong Provincial Science and Technology Planning Program of China (Industrial High-Tech Field) under Project Contract no. 2016A010101036, and Sichuan Provincial Science and Technology Planning Program of China (Technology Supporting Plan) under Project Contracts no. 2016GZ0061.

References

[1] W. Yang, J. Zhou, Z. Yu, and L. Li, "Bandwidth- and gain-enhanced circularly polarized antenna array using sequential phase feed," *IEEE Antennas and Wireless Propagation Letters*, vol. 13, pp. 1215–1218, 2014.

[2] A. B. Smolders and H. J. Visser, "Low side-lobe circularly-polarized phased arrays using a random sequential rotation technique," *IEEE Transactions on Antennas and Propagation*, vol. 62, no. 12, pp. 6476–6481, 2014.

[3] T.-Y. Han, "Series-fed microstrip array antenna with circular polarization," *International Journal of Antennas and Propagation*, vol. 2012, Article ID 681431, 5 pages, 2012.

[4] P. Xu, Z. Yan, T. Zhang, and X. Yang, "Broadband circularly polarized slot antenna array using a compact sequential-phase feeding network," *Progress In Electromagnetics Research C*, vol. 47, pp. 173–179, 2014.

[5] P. S. Hall, "Feed radiation effects in sequentially rotated microstrip patch arrays," *Electronics Letters*, vol. 23, no. 17, pp. 877–878, 1987.

[6] P. S. Hall and C. M. Hall, "Coplanar corporate feed effects in microstrip patch array design," *IEE Proceedings*, vol. 135, no. 3, pp. 180–186, 1988.

[7] P. S. Hall, J. Huang, E. Rammos, and A. Roederer, "Gain of circularly polarised arrays composed of linearly polarised elements," *Electronics Letters*, vol. 25, no. 2, pp. 124–125, 1989.

[8] P. S. Hall, J. S. Dahele, and J. R. James, "Design principles of sequentially fed, wide bandwidth, circularly polarised microstrip antennas," *IEE Proceedings H: Microwaves, Antennas and Propagation*, vol. 136, no. 5, pp. 381–389, 1989.

[9] P. S. Hall and M. S. Smith, "Sequentially rotated arrays with reduced sidelobe levels," *IEE Proceedings: Microwaves, Antennas and Propagation*, vol. 141, no. 4, pp. 333–336, 1994.

[10] J. Huang, "A technique for an array to generate circular polarization with linearly polarized elements," *IEEE Transactions on Antennas and Propagation*, vol. 34, no. 9, pp. 1113–1124, 1986.

[11] A. A. Kishk, "Performance of planar four-element array of single-fed circularly polarized dielectric resonator antenna," *Microwave and Optical Technology Letters*, vol. 38, no. 5, pp. 381–384, 2003.

[12] H. Evans, P. Gale, B. Aljibouri, E. G. Lim, E. Korolkwiwicz, and A. Sambell, "Application of simulated annealing to design of serial feed sequentially rotated 2/spl times/2 antenna array," *Electronics Letters*, vol. 36, no. 24, pp. 1987–1988, 2000.

[13] A. Chen, Y. Zhang, Z. Chen, and C. Yang, "Development of a Ka-band wideband circularly polarized 64-element microstrip antenna array with double application of the sequential rotation feeding technique," *IEEE Antennas and Wireless Propagation Letters*, vol. 10, pp. 1270–1273, 2011.

[14] V. Rafii, J. Nourinia, C. Ghobadi, J. Pourahmadazar, and B. S. Virdee, "Broadband circularly polarized slot antenna array using sequentially rotated technique for C-band applications," *IEEE Antennas and Wireless Propagation Letters*, vol. 12, pp. 128–131, 2013.

[15] Y. Lu, D. G. Fang, and H. Wang, "A wideband circularly polarized 2×2 sequentially rotated patch antenna array," *Microwave and Optical Technology Letters*, vol. 49, no. 6, pp. 1405–1407, 2007.

[16] S.-L. S. Yang, R. Chair, A. A. Kishk, K.-F. Lee, and K.-M. Luk, "Study on sequential feeding networks for subarrays of circularly polarized elliptical dielectric resonator antenna," *IEEE Transactions on Antennas and Propagation*, vol. 55, no. 2, pp. 321–333, 2007.

[17] S.-K. Lin and Y.-C. Lin, "A compact sequential-phase feed using uniform transmission lines for circularly polarized sequential-rotation arrays," *IEEE Transactions on Antennas and Propagation*, vol. 59, no. 7, pp. 2721–2724, 2011.

[18] D. M. Pozar, *Microwave Engineering*, John Wiley & Sons, Inc, New York, NY, USA, 3rd edition, 2005.

[19] Ansoft HFSS, "version 2013," http://www.ansys.com.

[20] C. A. Balanis, *Antenna Theory: Analysis and Design*, John Wiley & Sons, Hoboken, NJ, USA, 2005.